THE ASTROPHYSICAL JOURNAL, 346:808–822, 1989 November 15

NEUTRON STAR EVOLUTION WITH INTERNAL HEATING

NORIAKI SHIBAZAKI
Department of Physics, Rikkyo University
AND
FREDERICK K. LAMB
Departments of Physics and Astronomy, University of Illinois at Urbana-Champaign
Received 1988 November 14; accepted 1989 March 9

ABSTRACT

Soon after a neutron star forms, a large fraction of the neutrons are expected to become superfluid. In current models, only the neutron superfluid in the inner crust is weakly coupled to the rest of the star. In solitary neutron stars that are being spun down by external torques, this superfluid is expected to be rotating faster than the rest of the star. Frictional interaction with the crust dissipates the free energy of superfluid differential rotation, heating the star. The thermal evolution predicted by current superfluid-crust interaction models is quite different from the evolution predicted by models without internal heating and previous models of heating. Heating rates near the maximum expected can significantly increase the photon luminosity of the star in the neutrino cooling era and dramatically alter the thermal evolution in the photon cooling era. Even quite small heating rates can greatly increase the temperature in the photon cooling era, qualitatively changing the thermal evolution. Standard cooling models are consistent with current pulsar temperature estimates and upper limits, except those for the Vela pulsar, which are lower than predicted. The superfluid differential rotations typically implied or allowed by standard cooling models range from very small to very large, depending on the pulsar. Nonstandard cooling models are consistent with existing temperature upper limits, even for high rates of internal heating. However, these models predict surface temperatures lower than those reported in several pulsars, even if internal heating rates are very high. Exponential decay of the external braking torque causes the surface temperature of an internally heated neutron star to fall exponentially. However, the available evidence suggests that torque decay occurs only after $\sim 10^7$ yr. If so, neutron stars as old as 10^6 yr may have surface temperatures as high as 6×10^5 K, and may therefore be detectable in soft X-rays. The thermal flux from nearby old pulsars may also be observable in the extreme UV with future instruments.

Subject headings: dense matter — pulsars — stars: evolution — stars: interiors — stars: neutron — stars: rotation

I. INTRODUCTION

An understanding of the rotational, thermal, and magnetic field evolution of neutron stars is necessary in order to interpret observations of rotation and accretion powered pulsars and other neutron stars correctly. Conversely, studies of the spin rates, surface temperatures, and magnetic fields of such objects provide information about the internal structure of neutron stars and their electrical, thermal, and dynamical properties.

The spin-down of strongly magnetic neutron stars was predicted prior to the discovery of pulsars (Pacini 1967). Once pulsars were discovered, their gradual slowing down was quickly interpreted as evidence that they have strong magnetic fields (see Manchester and Taylor 1977). More recent studies indicate that the dipole magnetic moments of pulsars align and/or decay on a time scale $\sim 10^7$ yr (see Lyne, Manchester, and Taylor 1985; Blair and Candy 1989; Dewey 1989).

Neutron superfluidity in neutron stars was also predicted before pulsars were discovered (Migdal 1959; Ginzburg and Kirzhnits 1965). Soon after the discovery that the pulse frequency of the Vela pulsar relaxes slowly following a glitch (Radhakrishnan and Manchester 1969; Reichley and Downs 1969), this behavior was interpreted as evidence that neutrons in the interiors of neutron stars are indeed superfluid (Baym *et al.* 1969). The discovery of a succession of glitches and complex postglitch frequency behavior in the Vela and other pulsars has stimulated an intensive effort to understand this frequency behavior in terms of the rotational properties of neutron stars (see Lamb 1985; Pines and Alpar 1985).

The discovery of compact galactic X-ray sources prompted the first studies of the thermal properties of newly formed neutron stars (Tsuruta and Cameron 1965). In recent years, detailed cooling calculations have been reported by several authors (Glen and Sutherland 1980; Van Riper and Lamb 1981; Nomoto and Tsuruta 1981, 1987; Richardson *et al.* 1982; see Tsuruta 1986 for a recent review). Careful comparisons of these calculations with optical and X-ray observations have constrained the structure and thermal properties of neutron stars but have not yet confirmed any particular model (see Helfand 1983).

Although most studies have treated them separately, the magnetic, rotational, and thermal properties of neutron stars are not independent. Instead, these properties all affect one another, as illustrated by the pioneering work of Greenstein (1975, 1976, 1979) and Harding, Guyer, and Greenstein (1978). For example, friction between differentially rotating components in the stellar interior heats the star, thereby changing its thermal evolution. Conversely, the internal temperature of

the star affects the amount of differential rotation. Both are influenced by evolution of the stellar magnetic field through its effect on the coupling of the neutron star interior to the crust and the coupling of the crust to the environment. The evolution of the stellar magnetic field is in turn influenced by the thermal evolution of the star.

The calculations of neutron star thermal and rotational evolution by Greenstein (1975) and Harding, Guyer, and Greenstein (1978) were based on the original two-component model of neutron stars (Baym *et al.* 1969), which neglects pinning of neutron superfluid vortices in the inner crust and assumes that the neutron superfluid in the fluid core is weakly coupled to the crust. Since these calculations were completed, new observational and theoretical results have changed the accepted picture of neutron star interiors (see Lamb 1985). Detailed analyses of pulse frequency changes following glitches have revealed complex behavior that is not adequately explained by the two-component model (Downs 1981; Lohsen 1981; Demianski and Proszynski 1983). Studies of the rotation powered pulsar in the Crab Nebula and the accretion powered pulsars Her X-1 and Vela X-1 have shown that these neutron stars respond to small-scale changes in rotation rate essentially like rigid bodies (Boynton and Deeter 1979; Boynton 1981; Boynton *et al.* 1984; Deeter *et al.* 1989). New theoretical calculations (Alpar, Langer, and Sauls 1984; see also Alpar and Sauls 1988) indicate that the neutron superfluid in the fluid core of a neutron star is tightly coupled to the crust. In this new picture, the only component of the star that is thought to be weakly coupled to the crust is the neutron superfluid in the inner crust.

These developments have focused increased attention on how the neutron superfluid in the inner crust interacts with other components of the star (Feibelman 1971; Packard 1972; Anderson and Itoh 1975; Ruderman 1976; Alpar 1977; Pines *et al.* 1980; Anderson *et al.* 1982; Alpar *et al.* 1984*a*; Epstein 1988; Epstein and Baym 1988; Bildsten and Epstein 1989). In many of the proposed models, the difference between the angular velocity of the superfluid and the angular velocity of the crust remains almost constant as the crust spins down. Friction between the superfluid and the crust dissipates the free energy of this differential rotation, heating the interior of the star. The effect of this heating on the temperature of a neutron star old enough to be in thermal balance in the photon cooling era has been discussed by Alpar *et al.* (1984*a*). However, the effect of internal heating on the thermal evolution of younger neutron stars, the time required to achieve thermal balance, the age at which photon cooling begins to dominate, and the effect of magnetic field evolution have not been investigated previously.

Here we report the results of a study of the implications of current superfluid-crust interaction models for the thermal evolution of neutron stars. Our calculations take into account the initial heat content of the star, spin-down of the star by an external braking torque, and the effect of torque decay caused by magnetic field alignment and/or decay. In § II we describe the physical ideas that motivated the present calculations and introduce the equations that describe the rotational, thermal, and magnetic field evolution of the star. In § III we introduce simple analytical models that describe the qualitative features of thermal evolution in the neutrino and photon cooling eras, present numerical results for two model stars that span the range of behaviors currently expected, and discuss the effects of magnetic field decay on the evolution. In § IV we compare our results with the results of previous calculations and discuss the constraints on models of the superfluid-crust interaction and neutron star cooling imposed by searches for thermal radiation from nearby pulsars. Our conclusions are summarized briefly in § V.

II. MODEL

a) Physical Picture

Shortly after they are formed, neutron stars are expected to develop several distinct regions (see Lamb 1985): (1) a surface, which may be solid or liquid, depending on the temperature of the star and the strength of its surface magnetic field; (2) an outer crust, consisting of a solid lattice of nuclei embedded in a sea of relativistic degenerate electrons; (3) an inner crust, consisting of a solid lattice of nuclei embedded in a sea of $^1S_0$ superfluid neutrons and relativistic electrons; (4) a fluid core, consisting mainly of a $^3P_2$ neutron superfluid but also including a dilute plasma of normal electrons and superconducting protons; and (5) possibly, in heavier stars, a distinct inner core, which might consist of condensed pions or matter in some other exotic state.

The neutron superfluids in a rotating neutron star are expected to form vortices (see Sauls 1989). The vortices in the neutron superfluid in the core of the star are thought to be strongly magnetized because the neutrons circulating around each vortex drag superfluid protons with them, creating a substantial proton current around the neutron vortex (Alpar, Langer, and Sauls 1984). Consequently, the neutron superfluid in the stellar core couples strongly to the electrons there. As a result, the rotation rate of the neutron superfluid in the core is expected to relax to the rotation rate of the crust in a time $\sim 4 \times 10^2$–10^4 P, where P is the rotation period of the star (Alpar and Sauls 1988). Thus, the neutron superfluid in the core may be treated as corotating with the crust on evolutionary time scales. These two components together account for $\gtrsim 90\%$ of the moment of inertia of the star.

In contrast to the neutron superfluid in the core, the neutron superfluid in the inner crust may have only a weak frictional interaction with the rest of the star. This superfluid accounts for $\lesssim 10\%$ of the stellar moment of inertia. Thus, the existence of weakly coupled superfluid in the inner crust is consistent with the results of pulse timing studies of the Crab pulsar, Her X-1, and Vela X-1, which indicate that these neutron stars are responding to small rotational disturbances as if they are essentially rigid bodies (Boynton and Deeter 1979; Boynton 1981; Boynton *et al.* 1984; Deeter *et al.* 1989).

In newly formed neutron stars, the hot neutron fluid in the inner crust is expected to be normal and hence to corotate with the crust. As the star cools below a critical temperature $\sim 10^9$–10^{10} K, the neutrons in the inner crust become superfluid, dramatically reducing the friction between them and the other components of the star (see Sauls 1989). As the star cools further, scattering of thermally excited normal neutrons in the vortex cores by electrons, phonons, impurities, and dislocations drops exponentially (Feibelman 1971; Harding, Guyer, and Greenstein 1978). Thus, the friction between the neutron superfluid and the other components of the inner crust at temperatures below $\sim 3 \times 10^7$ K is due largely to processes that are temperature independent, such as scattering of electrons by the charge induced around the vortices by the long-range portion of the vortex-nucleus interaction (Bildsten and

Epstein 1989). This process gives a superfluid-crust frictional coupling time ~ 1 yr. Other processes, such as the electron scattering induced by the short-range portion of the vortex-nucleus interaction and long-wavelength excitations of lattice modes by the vortex as a whole, may produce greater friction, but the rates of these processes have not yet been calculated.

While the difference in angular velocities remains sufficiently small, the interaction between the vortices and the lattice of nuclei in the inner crust may "pin" the vortices to the nuclei, to the spaces between nuclei, or to lattice defects (Anderson and Itoh 1975; Alpar 1977; Epstein and Baym 1988; Sauls 1989). In regions of the inner crust where the vortex lines are pinned, the angular velocity of the superfluid remains constant in time. Thus, as the crust spins down, there is a growing difference between the angular velocity of the array of pinned vortices, which rotates with the crust, and the angular velocity of the neutron superfluid, which is rotating faster. This angular velocity difference produces a force on the vortex lines that is perpendicular to the rotation axis and directed outward (see Sauls 1989). The angular velocity difference is diminished if the vortex lines move radially outward.

Several authors have proposed mechanisms that might allow some or all of the vortex lines in the inner crust to move outward. One possibility is that when the angular velocity difference exceeds some threshold, the stress transmitted to the crust by the pinned vortices cracks the crust, allowing some of the vortex lines to move outward without unpinning (Ruderman 1976). Another possibility is that the vortices in a portion of the inner crust suddenly unpin when the angular velocity difference exceeds some critical value; once unpinned, friction between the neutron superfluid and the other components of the inner crust would cause them to move outward (Anderson and Itoh 1975; Pines *et al.* 1980). Alternatively, when the angular velocity difference exceeds a certain critical value, the flow of superfluid neutrons around and through the nuclei may become dissipative (Epstein 1988). Thermal excitation of vortices that are sufficiently weakly pinned may cause them to overcome occasionally the potential energy barrier that pins them, if the force on the vortices is sufficiently large (Alpar *et al.* 1984*a*); once unpinned, frictional interaction with the other components of the inner crust would cause them to move outward. A model involving such thermally activated vortex creep has been proposed to explain the post-glitch frequency behavior observed in the Vela, Crab, and other pulsars (Alpar *et al.* 1984*b*; Alpar, Nandkumar, and Pines 1985). However, if the 620-day quasi-periodic pulse phase variations recently reported in the Crab pulsar (Lyne, Pritchard, and Smith 1988) are due to small-amplitude free-precession, only a tiny fraction of the superfluid in the inner crust can be pinned (Jones 1988; see also Shaham 1977). For recent reviews of superfluidity in neutron stars, see Alpar and Pines (1989) and Sauls (1989).

All of the mechanisms just mentioned share three basic features: (1) the vortices in the inner crust move outward when the angular velocity difference exceeds some critical value (the outward motion may be sudden, as in glitches, or gradual, as in vortex creep); (2) the outward motion allows the angular velocity of the neutron superfluid to follow the spin-down of the other components of the neutron star on evolutionary time scales; and (3) as the vortices move outward, the differential rotational energy of the superfluid is dissipated, heating the interior of the star.

In the following sections we explore the effects of the heating predicted by this class of superfluid-crust interaction models on the thermal evolution of solitary neutron stars, using a multiple-component model of the star. In this model we assume that all the matter in the star other than the neutron superfluid in the inner crust has a constant moment of inertia I_c (Baym 1981) and rotates uniformly with angular velocity Ω_c (Alpar and Sauls 1988). Only the free energy of the superfluid in the inner crust that is frictionally coupled to the rest of the star and therefore participates in the spin down of the star can be converted into heat. We assume that this superfluid can be treated as a sequence of components with constant moments of inertia I_i and time-varying angular velocities Ω_i (Alpar *et al.* 1984*a*). The total moment of inertia of the frictionally coupled superfluid in the inner crust is then

$$I_s \equiv \sum_i I_i \,. \tag{1}$$

We assume further that the differences

$$\omega_i \equiv \Omega_i - \Omega_c \tag{2}$$

between the angular velocities of the various neutron superfluid components and the crust are constant on evolutionary time scales, as would be the case if there is a critical angular velocity difference ω_i for each layer of superfluid which, if exceeded, leads to outward motion of the vortices in the layer. The angular momentum in the differential rotation of the frictionally coupled superfluid is then

$$J \equiv \sum_i I_i \omega_i \,. \tag{3}$$

We neglect any heating produced by processes other than dissipation of the rotational energy of the superfluid in the inner crust. Finally, we treat the rotational and thermal evolution of the star in the Newtonian approximation.

The critical angular velocity differences ω_i are expected to depend sensitively on highly uncertain details of the vortex-lattice interaction (see Alpar and Pines 1989; Sauls 1989). If the typical neutron gap energy is ~ 1 MeV, as originally estimated by Hoffberg *et al.* (1970), plausible assumptions about pinning to individual nuclei give $\omega_i \sim 10$ rad s^{-1}, except perhaps in certain regions of the inner crust where the pinning force, and hence ω_i, may be up to 10 times smaller (Sauls 1989). More recent calculations (Takatsuka 1984; Chen *et al.* 1986; Ainsworth, Pines, and Wambach 1989) have produced estimates of typical neutron gap energies as small as 0.2–0.5 MeV. If glitches are due to global vortex unpinning, ω_i must be $\sim 10^{-2}$ rad s^{-1} in a region of superfluid that has a moment of inertia $\sim 10^{-2}$–10^{-3} times the total moment of inertia of the star. Critical angular velocities might be this small if vortices pin to small variations in the number of nuclei within the vortex core (Anderson *et al.* 1982) or to lattice defects (Sauls 1989). Alpar *et al.* (1984*b*) have discussed values of $\omega_i \ll 0.1$, ~ 0.1–1, and $\gg 1$ rad s^{-1}, which they call superweak, weak, and strong pinning, respectively. Because of uncertainty about the neutron gap energy, the vortex pinning energy, and the structure of neutron stars, we explore the consequences of a range of J values, corresponding to $I_s/I \sim 2 \times 10^{-3}$–$10^{-1}$ and critical angular velocities $\omega_i \sim 10^{-2}$–10 rad s^{-1}. For simplicity, in the following sections we refer to the neutron superfluid in the inner crust as

"the superfluid" and to all other matter in the star as "the crust," unless otherwise noted.

As mentioned above, superfluid-crust angular velocity differences arise because the rotation of the stellar crust is slowed by an external torque. Thus, any change in the braking torque will affect the rotational and thermal evolution of the star. According to the conventional picture of solitary pulsars, the braking torque is due to emission of electromagnetic waves and particles by the star. This emission depends on the strength of the stellar magnetic field (see Manchester and Taylor 1977; Blair and Candy 1989; Dewey 1989).

Blandford, Applegate, and Hernquist (1983) have suggested that the magnetic fields of pulsars may grow with time. Such growth, if it occurs, is likely to take place early in the life of the pulsar, when the heat generated by dissipation of the differential rotation of the superfluid is small compared to the initial heat content of the star; hence, the effect on the thermal evolution of the star of any growth of its magnetic field is likely to be modest. We therefore neglect this possibility in our calculations.

There is strong evidence for eventual decay of the external braking torque. Whether this is interpreted as due to magnetic field alignment (Candy and Blair 1986; Blair and Candy 1989) or magnetic field decay (Gunn and Ostriker 1970; Lyne, Manchester, and Taylor 1985), the inferred decay time scale τ_d is $\sim 10^7$ yr. Because torque decay takes place relatively late in the life of a pulsar, it can profoundly affect the star's dynamical and thermal evolution. We therefore consider the effects of exponential torque decay with a time constant τ_d.

b) *Rotational Evolution Equations*

Interaction of the rotating neutron star with its environment causes its angular momentum to change, that is,

$$I_c \dot{\Omega}_c + \sum_i I_i \dot{\Omega}_i = N_{\rm ext} . \tag{4}$$

For the reasons discussed above, we explore the consequences of a general braking law of the form

$$N_{\rm ext} = -K\Omega_c^k , \tag{5}$$

where k is assumed constant. In order to explore the possible effects of magnetic field evolution, we allow K to vary with time according to the equation

$$K = K_0 e^{-t/\tau_d} , \tag{6}$$

where K_0 is a constant that describes the initial magnetic field orientation and strength, τ_d is the torque decay time constant, and t is the time since the star was formed. If torque decay is due to magnetic field decay, the magnetic energy will be converted into heat. For magnetic field strengths $\sim 10^{12}$ G, the heat generated as the field decays is $\sim 10^{-4}$ times the heat content of the star at the beginning of the photon cooling era, and hence can be safely neglected.

The constancy of ω_i on evolutionary time scales implies that the superfluid components and the crust are in rotational equilibrium on these time scales, that is

$$\dot{\Omega}_i = \dot{\Omega}_c . \tag{7}$$

Even if some rotational disequilibrium develops from time to time, the thermal evolution of the star will be unaffected as long as rotational equilibrium is restored in a time short compared to the thermal relaxation time. With equation (7), equation (4) expressing angular momentum conservation becomes simply

$$I\dot{\Omega}_c = N_{\rm ext} , \tag{8}$$

where

$$I = I_c + \sum_i I_i = I_c + I_s \tag{9}$$

is the total moment of inertia of the star.

Equation (8), with $N_{\rm ext}$ given by equations (5) and (6), can be integrated analytically. The result is

$$\Omega_c(t) = \frac{\Omega_{c1}}{\{1 + (\tau_d/\tau_{c1})[1 - e^{-(t-t_1)/\tau_d}]\}^{1/(k-1)}} , \tag{10}$$

where Ω_{c1} is the angular velocity of the crust and τ_{c1} is the characteristic age

$$\tau_c \equiv \frac{\Omega_c}{(k-1)|\dot{\Omega}_c|} = \frac{I}{(k-1)K\Omega_c^{k-1}} , \tag{11}$$

at time t_1. In the absence of torque decay, a pulsar's true age is approximately equal to its characteristic age if its initial angular velocity was much greater than its current angular velocity. In the presence of torque decay, the characteristic age is an overestimate of the true age.

c) *Thermal Evolution Equations*

In following the thermal evolution of the star, we assume that its interior (the region at densities $\rho \geq 10^{10}$ g cm^{-3}) is isothermal at $t \gtrsim 10^3$ yr. When there is no internal heating, this is a good approximation after a few years, if the equation of state of neutron matter is soft (Richardson *et al.* 1982; Nomoto and Tsuruta 1987). For a moderately stiff equation of state, the interior becomes approximately isothermal after $\sim$500–700 yr. If the equation of state is quite stiff, the interior may not become closely isothermal until $\sim 10^5$ yr (Nomoto and Tsuruta 1987). However, even in these latter cases the isothermal approximation introduces errors of less than 30% in the surface temperature and less than a factor 2.5 in the photon luminosity, after 0.3 yr. Errors of this size are smaller than the uncertainties in the temperature and luminosity introduced by the uncertainties in the superfluid-crust interaction.

We do not expect the validity of the isothermal core approximation to be affected by internal heating. In standard cooling models, the interior of the neutron star cools primarily via crust neutrino bremsstrahlung at the earliest times of interest to us (see Nomoto and Tsuruta 1987). Energy is therefore lost from the region where it is generated and which contains most of the heat capacity of the star. Hence we expect the thermal evolution to be well-described by a single internal temperature. In nonstandard cooling models, heat is generated in the inner crust and lost primarily from the center of the star via pion-mediated neutrino emission (see Baym and Pethick 1979). An internal temperature gradient is therefore required to carry the energy flux from the crust to the center, but this gradient is quite small, because the thermal conductivity is very large.

To estimate the temperature difference between the inner crust and the center, we equate the thermal current to the neutrino luminosity, that is

$$4\pi R_c^2 \kappa \nabla T \approx L_\nu . \tag{12}$$

Here $R_c \sim 10$ km is the radius of the inner edge of the crust and κ is the thermal conductivity. Regardless of whether or not the neutrons and protons are superfluid, the thermal conductivity

in the fluid core is dominated by the electrons. The electron conductivity is (Flowers and Itoh 1979, 1981)

$$\kappa_e \approx 1.0 \times 10^{23}(\rho/10^{14}\ \mathrm{g\ cm^{-3}}) \times (10^8 K/T)\ \mathrm{ergs\ s^{-1}\ cm^{-1}\ K^{-1}}\ . \quad (13)$$

The required fractional temperature difference is therefore

$$\Delta T/T \sim 10^{-3}(L_\nu/10^{35}\ \mathrm{ergs\ s^{-1}})(\rho/10^{14}\ \mathrm{g\ cm^{-3}})\ . \quad (14)$$

Since the neutrino luminosities of our nonstandard cooling models are $\lesssim 10^{35}$ ergs s^{-1} at the times of interest, the fractional temperature difference between the inner crust and the center of the star is $\lesssim 10^{-3}$. Hence internal heating does not affect the validity of the isothermal core approximation.

The thermal evolution of a star with an isothermal interior can be described approximately by the equation

$$C_V \dot{T}_c = H - \Lambda_\nu - \Lambda_\gamma\ , \quad (15)$$

where C_V is the heat capacity of the star, T_c is the central temperature, H is the internal heating rate, and Λ_ν and Λ_γ are the neutrino and photon luminosities, respectively. We now consider in turn each of the terms in equation (15).

The heat capacity of the star resides in the degenerate normal matter and can therefore be written

$$C_V = aT_c\ , \quad (16)$$

where the coefficient a depends on the stellar model. At the earliest times of interest to us ($t \sim 10^3$ yr), the internal temperatures of stars with "standard" cooling are $\lesssim 10^9$ K. The neutrons in the inner crust are thought to have critical temperatures $\gtrsim 10^9$ K and hence are expected to be superfluid at these temperatures. The neutrons in the fluid core, on the other hand, may have critical temperatures as low as $\sim 3 \times 10^8$ K, and hence may not yet have condensed at 10^9 K. As these neutrons condense, the coefficient a in equation (16) decreases by a factor ~ 4 (see Van Riper and Lamb 1981). At the earliest times of interest to us, the internal temperatures of stars with "nonstandard" cooling are $\lesssim 10^7$ K and hence the neutrons in the inner crusts and cores of such stars will already be superfluid. Given the uncertainties in estimating critical temperatues, in this first study of the effects of superfluid-crust interaction on thermal evolution we assume that the neutrons in the inner crust and core are superfluid at the earliest times of interest. The electrons and the layer of normal neutrons near the crust-core boundary then contribute about equally to a, which is $\sim 10^{29}$ ergs K^{-2}.

The rate of internal heating caused by dissipation of the differential rotational energy of the neutron superfluid is

$$H = -\dot{E}_{\mathrm{rot}} - \dot{E}_{\mathrm{ext}}\ , \quad (17)$$

where

$$\dot{E}_{\mathrm{rot}} = I_c \Omega_c \dot{\Omega}_c + \sum_i I_i \Omega_i \dot{\Omega}_i \quad (18)$$

and

$$\dot{E}_{\mathrm{ext}} = -N_{\mathrm{ext}} \Omega_c\ . \quad (19)$$

Using equations (2), (3), (7), (8), and (10), the heating rate (eq. [17]) can be written as

$$H(t) = J|\dot{\Omega}_c(t)| = \frac{H_1 e^{-(t-t_1)/\tau_d}}{\{1 + (\tau_d/\tau_{c1})[1 - e^{-(t-t_1)/\tau_d}]\}^{k/(k-1)}}\ , \quad (20)$$

where

$$H_1 \equiv J|\dot{\Omega}_{c1}| = \frac{J\Omega_{c1}}{(k-1)\tau_{c1}} \quad (21)$$

is the internal heating rate at time t_1.

The dominant neutrino emission processes depend on the internal temperature and structure of the star, and on whether or not there is a pion condensate. As noted above, the dominant process in stiff stars at the evolutionary times of interest to us is neutrino bremsstrahlung in the crust. In soft stars with a pion condensate, the dominant process is pion-mediated neutrino emission from the core. The rates of both processes are proportional to T^6 (see Baym and Pethick 1979), and hence we can write the neutrino luminosity as

$$\Lambda_\nu = \lambda_\nu T_c^6\ , \quad (22)$$

choosing a value of the constant λ_ν that is appropriate for the structure of the star and the dominant neutrino emission process.

Photons are emitted from the stellar surface. We assume that the photon luminosity is given by Stefan's law, that is

$$\Lambda_\gamma = 4\pi R^2 \sigma T_s^4\ , \quad (23)$$

where R is the radius of the star, σ is the Stefan-Boltzmann constant, and T_s is the effective surface temperature of the star. In reality, the photon spectrum from the surface of a strongly magnetic neutron star will not be exactly a Planck spectrum and equation (23) will not describe precisely the relation between the luminosity and the temperature of the surface (Romani 1987; see also Van Riper 1988, and references therein). However, equation (23) is expected to be approximately correct. The uncertainties in the superfluid-crust interaction do not warrant a more accurate treatment at present.

We wish to express Λ_γ in terms of the internal temperature of the star. Recent studies of the envelopes of strongly magnetic neutron stars have shown that the enhancement in the heat flux due to quantum effects is modest and is almost canceled by the reduction in the flux due to the effect of the magnetic field on electron transport (Hernquist 1985; Van Riper 1988; Ventura 1989). Thus, the heat flux through the envelope of a strongly magnetic star probably differs little (less than a factor of 3) from the heat flux through the envelope of a nonmagnetic star. We therefore adopt the relation between the effective surface temperature T_s and the internal temperature T_c found by Gudmundsson, Pethick, and Epstein (1982, 1983; see also Hernquist and Applegate 1984) for nonmagnetic stars. This relation is

$$T_s = 0.93 \times 10^6 (M/M_\odot)^{1/4} \times (R/10^6\ \mathrm{cm})^{-1/2}(T_c/10^8\ \mathrm{K})^{0.55}\ \mathrm{K}\ , \quad (24)$$

where M is the mass of the star. Using this relation, the photon luminosity can be written as

$$\Lambda_\gamma = 1.4 \times 10^{15}(M/M_\odot) T_c^{2.2}\ \mathrm{ergs\ s^{-1}} \equiv \lambda_\gamma T_c^{2.2}\ . \quad (25)$$

Note that in the Newtonian approximation, Λ_γ is independent of the radius of the star. Equations (24) and (25) are probably accurate to within 30% and a factor of 3, respectively, for internal temperatures in the range 2×10^7–10^9 K. They become uncertain at higher temperatures, because no reliable calculations of envelope opacities exist for part of the required range of temperatures and densities, and at lower tem-

peratures, because the opacities and the equation of state are both unreliable (Gudmundsson, Pethick, and Epstein 1982; Van Riper 1988).

The thermal evolution of a given stellar model can be determined by integrating equation (15) from some starting time t_1, given T_{c1}, τ_d, and any two of the three parameters Ω_{c1}, K_0, and τ_{c1}.

III. RESULTS

a) Overview

We have calculated the magnetic, rotational, and thermal evolution of a variety of neutron star models, with and without internal heating. Table 1 lists the parameters of two models that illustrate the range of thermal properties and cooling processes we have considered. Model 1 was constructed using a stiff equation of state (Padharipande and Smith 1975; see also Pandharipande, Pines, and Smith 1976). There is no pion condensate in the core and, for the temperatures of interest to us, neutrino emission is dominated by bremsstrahlung in the crust. Model 2 was constructed using a relatively soft equation of state (Baym, Pethick, and Sutherland 1971). The core is assumed to contain a pion condensate, and neutrino emission is dominated by the pion-catalyzed URCA process. Both models have $M = 1.4\ M_\odot$, and hence $\lambda_\nu = 1.9 \times 10^{15}$ ergs s^{-1} K$^{-2.2}$ (see eq. [25]). The neutrons in the stellar core and the inner crust are assumed to be superfluid. The total moment of inertia of the superfluid in the inner crust is estimated to be ~ 0.14 and $\sim 2.5 \times 10^{-3}$ times the total moment of inertia of the star, for models 1 and 2 respectively (Nandkumar 1985). These two models are representative of the "standard" and "nonstandard" cooling models considered by previous authors.

As explained in § II, only the free energy of the superfluid that is frictionally coupled to the crust is dissipated as the star slows down. Any superfluid that remains pinned is not frictionally coupled, does not participate in the spin down of the rest of the star, and produces no heat. The extent of frictional coupling depends on the rotational history of the star. For example, if the crustal angular velocity at the epoch of neutron condensation is much greater than all the critical angular velocities ω_i and the star is spinning down rapidly, the superfluid-crust angular velocity difference will quickly exceed all the ω_i, causing the superfluid to become frictionally coupled to the rest of the star. Conversely, if the crustal angular velocity at the epoch of neutron condensation is less than all the critical angular velocities ω_i, the superfluid-crust angular velocity difference will never exceed any ω_i, the superfluid will remain pinned, and there will be no internal heating. In intermediate cases, superfluid layers with small values of ω_i will become frictionally coupled early in the spin down of the star, whereas layers with large values of ω_i will become frictionally coupled later.

Current theoretical estimates give critical angular velocities $\omega_i \lesssim 10$ rad s^{-1}, as discussed in § II. Thus, all of the neutron superfluid in the inner crust of a solitary neutron star formed with an initial angular velocity $\Omega_{c0} \gg 10$ rad s^{-1} (initial period $P_0 \ll 0.6$ s) is likely to be frictionally coupled by the time the spin rate has decreased to ~ 10 rad s^{-1}. However, there is increasing evidence that many solitary pulsars, particularly those with strong magnetic fields, are born with initial angular velocities ~ 5–10 rad s^{-1} (see Narayan 1987 and references therein). The neutron superfluid in regions of these pulsars where ω_i is ~ 10 rad s^{-1} may remain permanently pinned.

The internal heating rate is $J|\dot{\Omega}_c|$, where J is the total differential angular momentum of the *frictionally coupled* superfluid layers (see eqs. [3] and [20]). It is therefore convenient to parameterize the effect of the superfluid on the thermal evolution of the star by J. On the other hand, the quantities that can be compared most directly with microscopic calculations are the critical angular velocity differences ω_i (Alpar *et al.* 1984*a*; Pines and Alpar 1985; Sauls 1989). Although the ω_i cannot be determined individually from J, if the total moment of inertia I_s of the frictionally coupled superfluid is known, we can estimate the *mean* critical angular velocity

$$\bar{\omega} \equiv \sum_i I_i \omega_i / \sum_i I_i = J/I_s \,. \tag{26}$$

However, the size of I_s for a given stellar model depends on its rotational history as well as the neutron energy gap as a function of density and other factors. As a result, estimates of I_s are rather uncertain. Therefore, in the discussion that follows we quote both J and $\bar{\omega}$, where relevant, using estimates of the *total* moment of inertia of the superfluid in the inner crust to convert from J to $\bar{\omega}$.

The thermal evolution predicted by current models of the superfluid-crust interaction is illustrated by the cooling curves shown in Figures 1 and 2. These curves were obtained by numerically integrating the thermal evolution equation (15) for stellar models 1 and 2, respectively, assuming $k = 3$, no torque evolution, and constant J. The evolutions were started at $t_1 = 100$ yr, with $T_{c1} = 10^{9.0}$ K, $\Omega_{c1} = 374$ rad s^{-1}, and $\tau_{c1} = 400$ yr (Fig. 1) and $T_{c1} = 10^{7.7}$ K, $\Omega_{c1} = 340$ rad s^{-1}, and $\tau_{c1} = 400$ yr (Fig. 2). The value of T_{c1} for Figure 1 was chosen to be close to the central temperature reported at 100 yr by Nomoto and Tsuruta (1987) for their 1.4 $M_\odot$ PS model S with standard cooling, while the value of T_{c1} for Figure 2 was chosen to be similar to the central temperature reported at 100 yr by Richardson *et al.* (1982) for their 1.33 $M_\odot$ model V. However, for the times of interest to us ($t \gtrsim 10^3$ yr), the thermal evolution is insensitive to the central temperature at 100 yr, unless unreasonably low values ($T_{c1} < 10^9$ K for model 1 and $T_{c1} < 10^7$ K for model 2) are chosen. The values of k and τ_{c1} chosen for the evolutionary calculations plotted in Figures 1 and 2 correspond to braking by vacuum magnetic dipole radiation, for perpendicular dipole components of 5×10^{30} and 3×10^{30} G cm^3, respectively. The values of Ω_{c1} are sufficiently large and the values of τ_{c1} sufficiently small that all of the superfluid in the inner crust may be treated as frictionally coupled at t_1. The

TABLE 1

NEUTRON STAR MODELS

Stellar Parameter	Model 1 (Standard Cooling)	Model 2 (Nonstandard Cooling)
$M\ (M_\odot)$	1.4	1.4
R (km)	15.8[a]	7.4[b]
I (g cm^2)	2.18×10^{45}[a]	6.51×10^{44}[b]
I_s (g cm^2)	3×10^{44}[c]	1.7×10^{42}[c]
a (ergs K^{-2})	2.0×10^{29}[d]	2.9×10^{29}[e]
λ_ν (ergs s^{-1} K^{-6})	4.3×10^{-17}[f]	3×10^{-9}[g]
T_{c2} (K)	2.1×10^8	1.8×10^6
T_{s2} (K)	1.2×10^6	1.3×10^5

[a] Pandharipande and Smith 1975. [b] Baym, Pethick, and Sutherland 1971. [c] Nandkumar 1985. [d] Van Riper and Lamb 1981. [e] Richardson *et al.* 1982. [f] Nomoto and Tsuruta 1987. [g] Maxwell 1978.

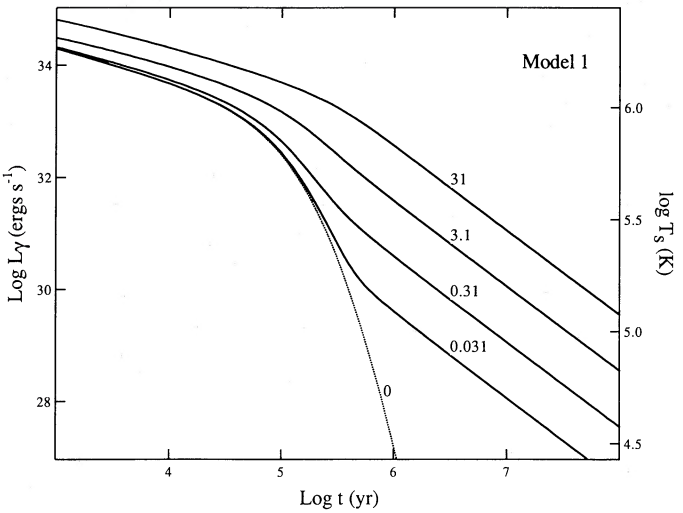

FIG. 1.—Evolutionary tracks for stellar model 1, illustrating the behavior of "standard" cooling models with and without internal energy dissipation. Model 1 is based on a relatively stiff equation of state and assumes no pion condensate in the stellar core. L_γ, T_s, and t are the photon luminosity, effective surface temperature, and age of the star. Dotted curve shows the thermal history in the absence of internal energy dissipation. Solid curves show the thermal histories produced by various rates of internal heating due to friction between the neutron superfluid and the crust. As explained in the text, the heating rate is governed by the differential angular momentum J of the neutron superfluid in the inner crust. The evolutionary tracks are labeled with the assumed value of J_{44}, the value of J in units of 10^{44} g cm^2 rad s^{-1}.

evolution from these initial conditions was followed for several values of J in the range predicted by current superfluid-crust interaction models. Each evolutionary track is labeled with the value of J assumed. The temperatures and luminosities become increasingly uncertain as T_s falls below $\sim 3 \times 10^5$ K, because relation (24) becomes increasingly unreliable below this temperature. The internal temperatures, surface temperatures, photon luminosities, and neutrino luminosities at selected times are listed in Tables 2 and 3.

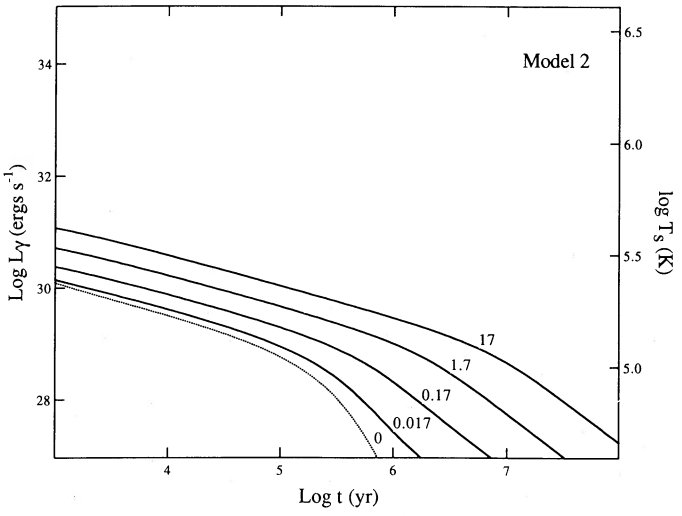

FIG. 2.—Evolutionary tracks for stellar model 2, illustrating the behavior of "nonstandard" cooling models with and without internal energy dissipation. Model 2 is based on a relatively soft equation of state and assumes a pion condensate in the stellar core. Conventions are the same as in Fig. 1. The evolutionary tracks with internal energy dissipation are labeled with the assumed value of the parameter J_{42}, the value of J in units of 10^{42} g cm^2 rad s^{-1}.

The evolutionary tracks of stars with internal heating display the same two distinct cooling eras seen in the evolutionary tracks of stars without internal heating. At early times, when the star is relatively hot, it cools mostly by neutrino emission. Later, when the star is colder, it cools primarily by emission of photons from its surface. The early, relatively flat parts of the cooling curves shown in Figures 1 and 2 correspond to the neutrino cooling era, whereas the later, more steeply falling parts of the curves correspond to the photon cooling era. We denote the time of transition to the photon cooling era by t_2. The central temperature at the time of transition is (see eqs. [22] and [25])

$$T_{c2} \equiv (\lambda_\gamma/\lambda_\nu)^{1/3.8} = 9.6 \times 10^3 (M/M_\odot)^{1/3.8} \lambda_\nu^{-1/3.8} \text{ K} . \quad (27)$$

This temperature is 2.1×10^8 K for model 1 and 1.8×10^6 K for model 2. The surface temperature T_{s2} at the time of transition is 1.2×10^6 for model 1 and 1.3×10^5 K for model 2. For the evolutionary tracks shown in Figure 1, the photon cooling era begins after 10^4–10^5 yr, depending on the value of J, while for the tracks shown in Figure 2, the transition to photon cooling is not reached until 5×10^4–4×10^6 yr. The wide range of transition times is due to the substantial delay in the onset of the photon cooling era when J is large, particularly for the nonstandard cooling model.

TABLE 2

THERMAL EVOLUTION OF MODEL 1

log t (yr)	log T_c (K)	log T_s (K)	log L_γ (ergs s^{-1})	log L_ν (ergs s^{-1})
		$J = 0$		
3.00.....	8.65	6.26	34.3	35.5
3.50.....	8.51	6.19	34.0	34.7
4.00.....	8.36	6.10	33.7	33.8
4.50.....	8.16	6.00	33.2	32.6
5.00.....	7.79	5.79	32.4	30.4
5.50.....	6.95	5.33	30.6	25.4
6.00.....	5.44	4.50	27.2	16.3
		$J = 3.1 \times 10^{43}$ g cm^2 rad s^{-1}		
3.00.....	8.66	6.27	34.3	35.6
3.50.....	8.53	6.20	34.0	34.8
4.00.....	8.39	6.12	33.7	34.0
4.50.....	8.21	6.02	33.3	32.9
5.00.....	7.90	5.85	32.6	31.0
5.50.....	7.37	5.56	31.5	27.9
6.00.....	6.96	5.34	30.6	25.4
6.50.....	6.61	5.14	29.8	23.3
7.00.....	6.27	4.95	29.1	21.2
7.50.....	5.92	4.76	28.3	19.2
8.00.....	5.58	4.58	27.6	17.1
		$J = 3.1 \times 10^{45}$ g cm^2 rad s^{-1}		
3.00.....	8.88	6.39	34.8	36.9
3.50.....	8.77	6.33	34.6	36.3
4.00.....	8.65	6.27	34.3	35.6
4.50.....	8.52	6.19	34.0	34.8
5.00.....	8.37	6.11	33.7	33.9
5.50.....	8.17	6.00	33.2	32.6
6.00.....	7.86	5.83	32.6	30.8
6.50.....	7.52	5.64	31.8	28.7
7.00.....	7.17	5.45	31.0	26.7
7.50.....	6.83	5.26	30.3	24.6
8.00.....	6.49	5.08	29.6	22.6

TABLE 3

THERMAL EVOLUTION OF MODEL 2

log t (yr)	log T_c (K)	log T_s (K)	log L_γ (ergs s^{-1})	log L_ν (ergs s^{-1})
		$J = 0$		
3.00.....	6.73	5.38	30.1	31.9
3.50.....	6.60	5.30	29.8	31.0
4.00.....	6.50	5.23	29.5	30.3
4.50.....	6.32	5.15	29.2	29.4
5.00.....	6.13	5.04	28.8	28.3
5.50.....	5.80	4.86	28.0	26.3
6.00.....	5.05	4.45	26.4	21.8
		$J = 1.7 \times 10^{41}$ g cm^2 rad s^{-1}		
3.00.....	6.87	5.45	30.4	32.7
3.50.....	6.76	5.39	30.1	32.0
4.00.....	6.64	5.32	29.9	31.3
4.50.....	6.51	5.25	29.6	30.5
5.00.....	6.37	5.18	29.3	29.7
5.50.....	6.20	5.08	28.9	28.7
6.00.....	5.93	4.94	28.3	27.0
6.50.....	5.57	4.74	27.5	24.9
7.00.....	5.22	4.54	26.8	22.8
7.50.....	4.88	4.36	26.0	20.7
8.00.....	4.53	4.17	25.2	18.7
		$J = 1.7 \times 10^{43}$ g cm^2 rad s^{-1}		
3.00.....	7.18	5.62	31.1	34.6
3.50.....	7.07	5.57	30.8	33.9
4.00.....	6.96	5.50	30.6	33.2
4.50.....	6.83	5.43	30.3	32.5
5.00.....	6.71	5.36	30.0	31.7
5.50.....	6.58	5.29	29.8	31.0
6.00.....	6.45	5.22	29.5	30.2
6.50.....	6.29	5.14	29.1	29.3
7.00.....	6.08	5.02	28.7	28.0
7.50.....	5.78	4.85	28.0	26.2
8.00.....	5.44	4.67	27.2	24.1

While the thermal inertia term dominates the internal heating term in the thermal evolution equation ($C_V|\dot{T}_c| \gg H$), the evolution of the star depends on its thermal history. Once the internal heating term dominates, however, the star quickly approaches thermal balance. If J is constant on evolutionary time scales, the approach to thermal balance takes place on the heating time scale

$$\tau_H \equiv aT_c^2/H = aT_c^2/J|\dot{\Omega}_c| . \tag{28}$$

The heating time scale τ_{H1} at time t_1 is $3 \times 10^3\, J_{44}^{-1}$ yr for the tracks shown in Figure 1 and $10^3\, J_{42}^{-1}$ yr for the tracks shown in Figure 2, where J_{44} and J_{42} are the values of J in units of 10^{44} and 10^{42} g cm^2 rad s^{-1}, respectively. More generally, the heating time scales are $10^6\, J_{44}^{-1}\dot{\Omega}_{12}^{-1}T_{s6}^{3.64}$ yr for model 1 and $10^4\, J_{42}^{-1}\dot{\Omega}_{12}^{-1}T_{s5}^{3.64}$ yr for model 2, where $\dot{\Omega}_{12}$ is the deceleration rate in units of 10^{-12} rad s^{-2} and T_{s5} and T_{s6} are the surface temperatures in units of 10^5 and 10^6 K, respectively. Once the star is in thermal balance, its temperature and luminosity are determined by its deceleration rate, regardless of its history. We discuss thermal balance in the neutrino and photon cooling eras below.

The implications of various superfluid-crust interaction models can be explored by comparing the temperatures and luminosities they predict with observation. If the star has not yet achieved thermal balance, cooling curves like those shown in Figures 1 and 2 are required. The curves for evolution *without* internal heating can be compared to observations of any star, since they do not depend on the star's rotational history. On the other hand, curves for evolution *with* internal heating can be compared to observations only if they have been calculated with an initial spin rate and braking torque that give the deceleration rate measured at the present epoch. If the star is in thermal balance, its temperature and luminosity can be computed directly from the measured deceleration rate, and evolutionary calculations are unnecessary.

As a specific example, the vortex-creep model proposed by Alpar *et al.* (1984*a*) can be investigated by identifying the I_i with the moments of inertia of the neutron superfluid in the various proposed pinning layers and adopting values of ω_i equal to the proposed critical angular velocity differences. In the terminology of Alpar *et al.*, the curves in Figure 1 with $J_{44} \ll 0.31$, ~ 0.31–3.1, and $\gg 3.1$ correspond to "superweak," "weak," and "strong pinning." The curves in Figure 2 with $J_{42} \ll 0.17$, ~ 0.17–1.7, and $\gg 1.7$ correspond to these same pinning regimes.

We now analyze some of the key properties of the neutrino and photon cooling eras, neglecting torque evolution. The impact of torque decay is discussed at the end of this analysis.

b) *Neutrino Cooling Era*

When internal heating is unimportant, neutrino cooling causes the central temperature to decrease with time according to the expression

$$T_\nu(t) = \frac{T_{c1}}{[1 + 4(t - t_1)/\tau_{\nu 1}]^{1/4}} , \tag{29}$$

where T_{c1} and $\tau_{\nu 1}$ are the central temperature and the neutrino cooling time scale

$$\tau_\nu \equiv \frac{a}{\lambda_\nu T_c^4} \tag{30}$$

at the starting time t_1 of the evolution. For times $t - t_1 \gg t_{\nu 1}$,

$$T_{c\nu}(t) \approx \left(\frac{a}{4\lambda_\nu}\right)^{1/4}\left(\frac{1}{t}\right)^{1/4} . \tag{31}$$

Thus, at these times $T_{c\nu}$ does not depend on T_{c1}, and declines as $t^{-0.25}$.

As internal heating becomes more important, the star moves toward thermal balance. For the evolutions shown in Figures 1 and 2, thermal balance is reached before the end of the neutrino cooling era for $J_{44} > 0.31$ and $J_{42} > 0.017$, respectively. Once the star is in thermal balance, its central temperature evolves in time according to (see eqs. [20] and [22])

$$T_{c\nu}^*(t) \equiv (H/\lambda_\nu)^{1/6} = (H_1/\lambda_\nu)^{1/6}[1 + (t - t_1)/\tau_{c1}]^{-k/6(k-1)} . \tag{32}$$

For $k = 3$ and $t - t_1 \gg \tau_{c1}$,

$$T_{c\nu}^*(t) \approx \left(\frac{H_1}{\lambda_\nu}\right)^{1/6}\left(\frac{\tau_{c1}}{t}\right)^{1/4} . \tag{33}$$

The exponents of time in equations (29) and (32) generally are not the same, and hence the temperature does not evolve according to a simple power law in the presence of internal heating. Instead, the central temperature first falls according to equation (29) and then follows equation (32) as internal heating

becomes dominant. However, if $k = 3$, the internal heating rate, the rate of change of the heat content of the star, and the neutrino luminosity all evolve with time in the same way. Thus, in this case the internal temperature does decay as a power of time, once the initial value of the temperature is forgotten ($t \gtrsim 10^3$ yr), with a power law index that is independent of the amount of internal heating. This behavior is clearly evident in Figures 1 and 2.

We can obtain a simple analytical expression for the temperature evolution in this case by noting that if the photon luminosity is neglected, equation (15), with the heat capacity, internal heating rate, and neutrino luminosity given by expressions (16), (20), and (22), can be integrated analytically, giving

$$T_{cv}(t) = \frac{T_{c1}^*}{[1 + (t - t_1)/\tau_{c1}]^{1/4}}, \tag{34}$$

where T_{c1}^* is the root of the polynomial equation

$$\lambda_\nu (T_{c1}^*)^6 - (a/4\tau_{c1})(T_{c1}^*)^2 - H_1 = 0 . \tag{35}$$

If the internal temperature T_{c1} at time t_1 is greater than T_{c1}^*, the temperature relaxes on the neutrino cooling time scale to the value given by equations (34) and (35) and then evolves according to this expression. The neutrino cooling time scale at t_1 is 150 yr for the evolutionary tracks shown in Figure 1 and 0.5 yr for the tracks shown in Figure 2. Equation (34) predicts that for times $t - t_1 \gg \tau_{c1}$, the internal temperature decays as $t^{-0.25}$ while the photon luminosity declines as $t^{-0.55}$, regardless of the heating rate. This prediction agrees well with our numerical calculations.

Although the power law behavior of the photon luminosity does not depend on the heating rate for $k = 3$, the coefficient of the power law *does* depend on the heating rate, but only very weakly. The reason is that the neutrino luminosity is very sensitive to the internal temperature ($L_\nu \propto T_c^6$), whereas the photon luminosity is not ($L_\gamma \propto T_c^{2.2}$). Thus, $L_\gamma \propto T_c^{2.2} \propto H^{1.1/3}$ if the star is in thermal balance; if the star is not yet in thermal balance, the photon luminosity is even less sensitive to the heating rate.

These expectations are confirmed by the numerical results. Figure 1 shows that the internal heating predicted by existing models of the superfluid-crust interaction increases the photon luminosity of model 1 by less than a factor of 3 in the neutrino cooling era, even if J has the largest value currently thought possible. This is due both to the temperature sensitivity of the neutrino emission and the contribution of the initial heat content during this era. For model 2, on the other hand, the initial heat content is lost more rapidly and internal heating is therefore more important. Figure 2 shows that the largest internal heating rate considered increases the photon luminosity of model 2 by about an order of magnitude during the neutrino cooling era.

Once the star is in thermal balance, its internal temperature is

$$T_{cv}^* \equiv \left(\frac{J|\dot{\Omega}_c|}{\lambda_\nu}\right)^{1/6} = \begin{cases} 1.2 \times 10^8 \, J_{44}^{1/6} \dot{\Omega}_{12}^{1/6} \text{ K} & \text{(model 1)}, \\ 2.6 \times 10^6 \, J_{42}^{1/6} \dot{\Omega}_{12}^{1/6} \text{ K} & \text{(model 2)}. \end{cases} \tag{36}$$

The resulting surface temperatures and photon luminosites are

$$T_{sv}^* = \begin{cases} 8.7 \times 10^5 \, J_{44}^{1.1/12} \dot{\Omega}_{12}^{1.1/12} \text{ K} & \text{(model 1)}, \\ 1.6 \times 10^5 \, J_{42}^{1.1/12} \dot{\Omega}_{12}^{1.1/12} \text{ K} & \text{(model 2)}, \end{cases} \tag{37}$$

and

$$L_\gamma^* \equiv 4\pi R^2 \sigma (T_{sv}^*)^4 = \begin{cases} 1.0 \times 10^{33} J_{44}^{1.1/3} \dot{\Omega}_{12}^{1.1/3} \text{ ergs s}^{-1} & \text{(model 1)}, \\ 2.5 \times 10^{29} J_{42}^{1.1/3} \dot{\Omega}_{12}^{1.1/3} \text{ ergs s}^{-1} & \text{(model 2)}. \end{cases} \tag{38}$$

Equations (37) and (38) can be inverted to obtain expressions that can be used to estimate J, if the star is in thermal balance and if $\dot{\Omega}_c$ and either T_s or L_γ are known from observations. These expressions are

$$J = \begin{cases} 4.4 \times 10^{44} (T_s/10^6 \text{ K})^{12/1.1} \dot{\Omega}_{12}^{-1} \text{ g cm}^2 \text{ rad s}^{-1} & \text{(model 1)}, \\ 5.9 \times 10^{39} (T_s/10^5 \text{ K})^{12/1.1} \dot{\Omega}_{12}^{-1} \text{ g cm}^2 \text{ rad s}^{-1} & \text{(model 2)}, \end{cases} \tag{39}$$

and

$$J = \begin{cases} 9.1 \times 10^{43} (L_\gamma/10^{33} \text{ ergs s}^{-1})^{3/1.1} \dot{\Omega}_{12}^{-1} \text{ g cm}^2 \text{ rad s}^{-1} & \text{(model 1)}, \\ 7.9 \times 10^{40} (L_\gamma/10^{29} \text{ ergs s}^{-1})^{3/1.1} \dot{\Omega}_{12}^{-1} \text{ g cm}^2 \text{ rad s}^{-1} & \text{(model 2)}. \end{cases} \tag{40}$$

Notice that the inferred value of J is very sensitive to T_{sv} and somewhat sensitive to L_γ.

c) *Photon Cooling Era*

The internal heating predicted by current models of the superfluid-crust interaction completely changes the conventional picture of neutron star cooling in the photon cooling era. Without internal heating, the photon luminosity falls steeply, as indicated by the dotted lines in Figures 1 and 2. With internal heating, the star cools much more slowly and hence the cooling curve is much flatter, as indicated by the solid lines in these figures. *At ages greater than $\sim 10^6$ yr, even the models with very small values of J have photon luminosities more than an order of magnitude greater than the corresponding models without internal* heating.

Approximate analytical solutions for thermal evolution in the photon cooling era can be obtained as follows. In the absence of internal heating, the star simply loses its initial heat content by radiating photons. The cooling curve is therefore given approximately by balancing the thermal inertia and photon luminosity terms in the thermal evolution equation (15), with the result

$$T_{c\gamma}(t) = \frac{T_{c2}}{[1 + (t - t_2)/5\tau_{\gamma 2}]^5}, \tag{41}$$

where T_{c2} and $\tau_{\gamma 2}$ are the central temperature and the photon cooling time scale

$$\tau_\gamma \equiv \frac{a}{\lambda_\gamma T_c^{0.2}} = 8 \times 10^4 \left(\frac{a}{10^{29} \text{ ergs K}^{-2}}\right) \times \left(\frac{\lambda_\gamma}{10^{15} \text{ ergs s}^{-1} \text{ K}^{-2.2}}\right)^{-1} \left(\frac{T_c}{10^8 \text{ K}}\right)^{-0.2} \text{ yr} \tag{42}$$

at the starting time t_2 of the photon coding era. $\tau_{\gamma 2}$ is 7×10^4 yr for model 1 and 3×10^5 yr for model 2. For times $t - t_2 \gg \tau_{\gamma 2}$,

$$T_{c\gamma}(t) \approx T_{c2} \left(\frac{5\tau_{\gamma 2}}{t}\right)^5 = \left(\frac{5a}{\lambda_\gamma}\right)^5 \left(\frac{1}{t}\right)^5 . \tag{43}$$

Thus, at these times the internal temperature does not depend on its value T_{c2} at the start of the photon cooling era.

If J is appreciable, the internal heating term in the thermal evolution equation quickly dominates the thermal inertia term. The temperature of the star is then determined by a balance between internal heating and photon cooling. Balancing the rates given by equations (20) and (25) gives

$$T_{c\gamma}^{*}(t) \equiv \left(\frac{H}{\lambda_\gamma}\right)^{1/2.2} = \left(\frac{H_2}{\lambda_\gamma}\right)^{1/2.2}\left[1 + \frac{(t - t_2)}{\tau_{c2}}\right]^{-k/2.2(k-1)}, \tag{44}$$

where H_2 and τ_{c2} are the internal heating rate and characteristic age at t_2. For $k = 3$ and $t - t_2 \gg \tau_{c2}$,

$$T_{c\gamma}^{*}(t) \approx \left(\frac{H_2}{\lambda_\gamma}\right)^{1/2.2}\left(\frac{\tau_{c2}}{t}\right)^{3/4.4}. \tag{45}$$

The internal temperature evolution predicted by expressions (43) and (45) agrees fairly well with the numerical results shown in Figures 1 and 2. At times well into the photon cooling era, these expressions give $T_c \propto t^{-0.68}$ with internal heating and $T_c \propto t^{-5}$ without heating, showing clearly how dissipation of the superfluid rotational energy slows the cooling of older neutron stars.

If the star is in thermal balance in the photon cooling era, $L_\gamma = J|\dot{\Omega}_c|$. The corresponding central and surface temperatures are

$$T_{c\gamma}^{*} \equiv (J|\dot{\Omega}_c|/\lambda_\gamma)^{1/2.2} = 4.9 \times 10^6 J_{42}^{1/2.2}\dot{\Omega}_{12}^{1/2.2}\ \text{K} \quad \text{(models 1 and 2)}, \tag{46}$$

and

$$T_{s\gamma}^{*} \equiv \left(\frac{J|\dot{\Omega}_c|}{4\pi R^2\sigma}\right)^{1/4} = \begin{cases} 4.9 \times 10^5 J_{44}^{1/4}\dot{\Omega}_{12}^{1/4}\ \text{K} & \text{(model 1)}, \\ 2.3 \times 10^5 J_{42}^{1/4}\dot{\Omega}_{12}^{1/4}\ \text{K} & \text{(model 2)}. \end{cases} \tag{47}$$

Solving instead for J, one obtains expressions that can be used to estimate J, if $\dot{\Omega}_c$ and either L_γ or T_s are known from observations. These expressions are

$$J = L_\gamma/|\dot{\Omega}_c| = 10^{42}(L_\gamma/10^{30}\ \text{ergs s}^{-1})\dot{\Omega}_{12}^{-1}\ \text{g cm}^2\ \text{rad s}^{-1}, \tag{48}$$

and

$$J = \begin{cases} 1.8 \times 10^{45}(T_s/10^6\ \text{K})^4\dot{\Omega}_{12}^{-1}\ \text{g cm}^2\ \text{rad s}^{-1} \\ \qquad\qquad \text{(model 1)}, \\ 3.9 \times 10^{40}(T_s/10^5\ \text{K})^4\dot{\Omega}_{12}^{-1}\ \text{g cm}^2\ \text{rad s}^{-1} \\ \qquad\qquad \text{(model 2)}. \end{cases} \tag{49}$$

d) *Effect of Torque Decay*

In the previous development we have assumed that the torque coefficient K is constant in time. However, as discussed in § II, there is strong evidence that the braking torque on pulsars decays with a time constant $\tau_d \sim 10^7$ yr. If so, and if there is significant internal heating, almost all neutron stars will be in thermal balance in the photon cooling era ($t > t_2$) by the time the rotational deceleration rate begins to fall appreciably. Assuming $\tau_d \gg t_1$, $\tau_d \gg \tau_{c1}$, and $t \gg \tau_{c1}$, the central temperature evolves in time according to (see eqs. [20] and [25])

$$T_c(t) \approx \frac{(H_1/\lambda_\gamma)^{1/2.2}e^{-t/2.2\tau_d}}{[(\tau_{c1}/\tau_d)(1 - e^{-t/\tau_d})]^{k/2.2(k-1)}}. \tag{50}$$

Thus, for times $t - t_2 \gtrsim \tau_d$, the central temperature falls exponentially with time constant 2.2 τ_d, because the decay of the braking torque causes the star to decelerate more slowly, reducing the internal heating rate. However, as the heating rate falls, the heating time scale τ_H eventually exceeds the photon cooling time scale τ_γ, so that thermal balance no longer holds. The star then simply radiates away its existing thermal energy, and hence the central temperature decreases approximately according to equation (41), with t_2 replaced by the time t_3 at which internal heating becomes unimportant.

If τ_d is $\sim 10^7$ yr, as the available evidence suggests, evolutionary tracks calculated for internal heating without torque decay are a good approximation to the evolutionary tracks with decay, for times $t \lesssim 10^7$ yr. At 10^6–10^7 yr, stars with internal heating are much hotter than those without, so that even neutron stars this old may have surface temperatures $\sim 10^5$ K, and may therefore by detectable with future soft X-ray and extreme UV instruments. Even if τ_d is as small as 10^6 yr, the photon luminosity of stars that have internal heating should be much larger at 10^6 yr than the luminosity of stars that do not. Hence, if internal heating occurs, it should be detectable.

IV. DISCUSSION

a) *Comparison with Previous Calculations*

The surface temperature of model 1 without internal heating is within 20% at 10^4 yr and within a factor of 2 at 10^6 yr of the surface temperature reported by Nomoto and Tsuruta (1987) for their 1.4 $M_\odot$ PS model S with standard cooling. The surface temperature evolution of model 2 without internal heating joins smoothly to the surface temperature evolution reported by Richardson *et al.* (1982) in the interval from 10–100 yr (the last point reported by these authors) for their 1.33 $M_\odot$ model V with nonstandard cooling. Considering the simplicity of our models and the differences in the assumed properties of our models relative to these comparison models, this agreement appears satisfactory.

The thermal evolution of our models with internal heating is qualitatively different from the thermal evolution of the neutron star models constructed by Greenstein (1975) and Harding, Guyer, and Greenstein (1978). In our models, the temperature falls relatively slowly during the neutrino cooling era and then more steeply during the photon cooling era, although not as steeply as in the absence of internal heating. In the models of Greenstein *et al.*, on the other hand, the temperature falls slowly at early times and is almost independent of time at late times, so that all old neutron stars have essentially the same temperature.

Some of the difference in the thermal behavior of these two sets of models is due to different assumptions about the interaction between the neutron superfluid and the crust. For example, Greenstein *et al.* assumed that the neutron superfluid in the core couples to the crust only via electron scattering by the thermally excited normal neutrons in the vortex cores. They neglected vortex pinning in the inner crust and considered coupling of the neutron superfluid to the inner crust only via interaction of the crustal lattice with the thermally excited normal neutrons in the vortex cores. All the superfluid-crust coupling mechanisms considered by Greenstein *et al.* depend exponentially on the inverse of the internal temperature of the star, and hence are extremely sensitive to the internal temperature, for moderate to low temperatures.

However, the weak dependence of the temperature on age found by Greenstein *et al.* is due to their use of several approximations that are valid only briefly, if at all, during the evolution of the star. First, they neglected the initial heat content of the star. With this assumption, the only source of heat is internal energy dissipation. They also assumed that the star is in rotational equilibrium ($\dot{\Omega}_s = \dot{\Omega}_c$) and that the superfluid-crust angular velocity difference ω is proportional to $\dot{\Omega}_c \tau$, where τ is the superfluid-crust coupling time. The internal heating rate $I_s \dot{\Omega}_s \omega$ is then equal to $I_s \dot{\Omega}_c \omega$, and increases exponentially as the temperature decreases. As a result, the temperature in their models declines only logarithmically with time at late times.

Actually, the heat produced by the frictional superfluid-crust interactions considered by Greenstein *et al.* is more important than the initial heat content of the star only for times $\gtrsim 4 \times 10^5$ yr, for standard cooling, or $\gtrsim 10^5$ yr, for nonstandard cooling. Only at these times does the dissipation of differential rotational energy significantly affect the star's thermal evolution. On the other hand, the assumption that the star is in rotational equilibrium and that ω is proportional to $\dot{\Omega}_c \tau$ is only appropriate while the superfluid-crust coupling time τ, which increases as the star cools, remains shorter than the characteristic age τ_c. Once τ exceeds τ_c, the superfluid decouples from the crust, Ω_s becomes almost constant, and internal heating effectively ceases. Because τ is extremely sensitive to the temperature, this occurs quite suddenly. For the superfluid-crust interactions considered by Greenstein *et al.*, the superfluid decouples when the internal temperature falls below $\sim 10^7$ K. For stars of moderate mass, this occurs at $\sim 10^4$ to $\sim 10^5$ yr, depending on the amount of impurity scattering. Thus, by the time the thermal evolution could be affected by internal heating, the neutron superfluid is beginning to decouple from the crust. Thus, the approximations used by Greenstein *et al.* are justified only for a short time, if at all.

The thermal evolution calculations reported here are based on a physical picture that is quite different from the one assumed by Greenstein *et al.* As discussed in § II, recent observational and theoretical work strongly indicates that the neutron superfluid in the stellar core is actually tightly coupled to the crust on evolutionary time scales and that the only weakly coupled component is the neutron superfluid in the inner crust. Moreover, electron scattering off the positive charge induced by the long-range part of the vortex-nucleus interaction causes temperature independent friction that couples the inner crust and the neutron superfluid within it on a time scale ~ 1 yr. Other temperature independent interactions may produce even greater friction (other sources of friction are required if outward vortex motion is to account for the glitches observed in older neutron stars). Thus, once layers of neutron superfluid become frictionally coupled to the rest of the star on evolutionary time scales, they will remain coupled, even in very old stars.

Pinning of vortices in the inner crust prevents the strong frictional interaction from driving the mean superfluid-crust angular velocity difference $\bar{\omega}$ to a very small value. The combination of vortex pinning and strong friction maintains rotational equilibrium even in very old stars, with a crust-superfluid angular velocity difference that remains approximately constant once the internal temperature has fallen below a fairly high critical value (Alpar and Pines 1989). As a result, the internal heating rate is almost independent of the star's temperature, and hence the temperature declines steadily, although more slowly than if heating were absent, throughout the photon cooling era. If the external braking torque decays exponentially, the resulting decline in the angular deceleration of the star causes the internal heating rate and hence the temperature to fall exponentially on the torque decay time scale.

We caution that according to our evolutionary models, estimates of the surface temperature and luminosity which assume that the star is in the photon cooling era (Alpar *et al.* 1984*a*, *b*; Alpar, Nandkumar, and Pines 1985; Brinkmann and Ögelman 1987; Alpar *et al.* 1987; Alpar *et al.* 1988; Ögelman and Zimmerman 1987; Alpar, Cheng, and Pines 1989) are valid only after 10^4–10^5 yr, for standard cooling, or $5 \times 10^4 - 4 \times 10^6$ yr, for nonstandard cooling. The larger the mean differential rotation of the frictionally coupled neutron superfluid, the later the onset of the photon cooling era.

b) *Comparison with Observations*

The imaging instruments on the *Einstein Observatory* were used to search for thermal X-ray emission from neutron stars (see Helfand, Chanan, and Novick 1980; Helfand 1983; Seward 1987). Several of the pulsars detected in this search were subsequently studied using the *EXOSAT* observatory (Alpar *et al.* 1987; Brinkmann and Ögelman 1987; Ögelmann and Zimmerman 1989). In comparing our evolutionary calculations with these observations, we assume a braking torque with $k = 3$ and no torque decay, so that the characteristic age of a pulsar is $\tau_c = \Omega_c / |2\dot{\Omega}_c|$.

The *Einstein Observatory* survey gave X-ray luminosity upper limits in the range 0.5–5×10^{30} ergs s^{-1} for 10 pulsars within 500 pc of the Sun (Helfand 1983). Assuming these neutron stars are $\sim 10^6$ yr old, for our standard cooling model the highest upper limit implies $J \lesssim 3 \times 10^{43}$ g cm^2 rad s^{-1} or, equivalently, $\bar{\omega} \lesssim 0.1$ rad s^{-1}, whereas the lowest upper limit implies $J \lesssim 3 \times 10^{42}$ g cm^2 rad s^{-1} ($\bar{\omega} \lesssim 0.01$ rad s^{-1}). For stellar models based on softer equations of state, the limits on $\bar{\omega}$ are somewhat higher, because the superfluid moment of inertia I_s is smaller for these models. Thus, these upper limits are consistent with standard cooling. For our nonstandard cooling model, even the lowest of these upper limits is consistent with the maximum superfluid differential rotation currently thought possible.

The implications of observed temperatures or upper limits on the X-ray emission from the following pulsars deserve special comment:

PSR 0525+21.—Alpar, Nandkumar, and Pines (1985) have inferred that the internal temperature of this older pulsar is $\sim 1.4 \times 10^5$ K, on the basis of their vortex-creep model of postglitch pulse frequency behavior. At this internal temperature, both cooling models predict that the pulsar is cooling predominantly by photon emission (see Table 1). This conclusion is also consistent with our evolutionary calculations, if the true age of the pulsar is comparable to its characteristic age of 1.5×10^6 yr (Downs 1982). In the absence of internal heating, both our standard and nonstandard cooling models give internal temperatures lower than the value inferred by Alpar, Nandkumar, and Pines (see Tables 2 and 3). For the observed deceleration rate, our standard cooling model with heating (see eq. [46]) gives an internal temperature close to the inferred value for $J \sim 3 \times 10^{40}$ g cm^2 rad s^{-1} ($\bar{\omega} \sim 10^{-4}$ rad s^{-1}). Our nonstandard cooling model with heating gives an internal temperature close to this value for $J \sim 3 \times 10^{40}$ g cm^2 rad s^{-1} ($\bar{\omega} \sim 0.02$ rad s^{-1}). Thus, for either cooling model, quite small

values of the mean superfluid differential rotation are sufficient to produce the inferred internal temperature.

PSR 0531+21.—The *Einstein Observatory* results of Harnden and Seward (1984) imply that the Crab pulsar has a surface temperature less than 2.5×10^6 K, if its radius is 15 km. Our evolutionary calculations predict that the Crab pulsar is still in the neutrino cooling era at the present epoch. For our standard cooling model without internal heating, the predicted surface temperature at the present epoch is about 30% below the reported upper limit (see Table 2); with internal heating, the upper limit implies $J < 3 \times 10^{45}$ g cm^2 rad s^{-1} or $\bar{\omega} < 10$ rad s^{-1} (since $T_s \propto H^{1.1/12}$ in the neutrino cooling era, the surface temperature is very insensitive to the amount of superfluid differential rotation; see eq. [37]). For our nonstandard cooling model, even a heating rate many orders of magnitude greater than the maximum expected in current models is consistent with the temperature upper limit of Harnden and Seward.

On the basis of their model of postglitch frequency behavior, Alpar, Nandkumar, and Pines (1985) have estimated that the internal temperature of the Crab pulsar is $\sim 4 \times 10^8$ K. For our standard cooling model, this internal temperature implies a surface temperature that is about 30% less than the observed upper limit (see eq. [24]). In fact, evolution of our standard model without any heating gives an internal temperature at 940 yr quite close to the value inferred by Alpar, Nandkumar, and Pines, due to its initial heat content (see Table 2). However, a value of J as large as 3×10^{45} g cm^2 rad s^{-1} ($\bar{\omega}$ as large as 10 rad s^{-1}) gives an internal temperature only a factor ~ 2 higher, because of the weak dependence of internal temperature on heating rate in the neutrino cooling era (see eq. [36]). The implied surface temperature for this value of J would be marginally consistent with the upper limit of Harnden and Seward. For our nonstandard cooling model, internal heating rates many orders of magnitude greater than those of current superfluid-crust interaction models would be required to produce an internal temperature as high as that inferred by Alpar, Nandkumar, and Pines.

PSR 0656+14.—Córdova *et al.* (1989) have recently found evidence of soft X-ray emission from this pulsar, using the *Einstein Observatory* database. If the emission is blackbody radiation from the stellar surface, the radius of the star is no more than 16 km, and the distance to the pulsar is 400 pc, the HRI and IPC data imply that the surface temperature is in the range $3\text{–}6 \times 10^5$ K. For our standard cooling model, a pulsar with a surface temperature in this range is already in the photon cooling era (see Table 1). Our evolutionary calculations with standard cooling indicate that the initial heat content of the star is sufficient to produce a surface temperature near the upper end of the quoted range at a true age comparable to the pulsar's characteristic age of 1.1×10^5 yr (see Table 2); the differential angular momentum of the frictionally coupled superfluid component is therefore limited to $J \lesssim 3 \times 10^{42}$ g cm^2 rad s^{-1} or $\bar{\omega} \lesssim 0.01$ rad s^{-1} (see eq. [49]). For our nonstandard cooling model, a pulsar with a surface temperature in the reported range is still in the neutrino cooling era (see Table 1). Our evolutionary calculations with nonstandard cooling indicate that the initial heat content at 10^5 yr produces a surface temperature a factor of 3–6 less than the reported value (see Table 3); a mean superfluid differential angular momentum three orders of magnitude larger than expected in current models would be required to heat the surface to a temperature within the reported range (see eq. [39]).

PSR 0833−45.—Harnden *et al.* (1985) observed the X-ray point source at the position of the Vela pulsar using the *Einstein Observatory*. If the total point source flux is interpreted as blackbody emission from the neutron star surface, the surface temperature is $\sim 9 \times 10^5$ K. If instead the flux modulated at the pulsar spin period is used to derive a surface temperature, the temperature is $\lesssim 3 \times 10^5$ K. The point source has also been observed by Ögelman and Zimmerman (1989) using *EXOSAT*. Assuming that the total point source flux is blackbody-like emission from the surface of the neutron star, they find that the surface temperature is in the range $6\text{–}9 \times 10^5$ K for a star of radius 15 km, or in the range $7\text{–}10 \times 10^5$ K for a star of radius 8 km.

The initial heat content of our standard cooling model produces a surface temperature at 10^4 yr, the presumed age of the Vela pulsar, about 50% higher than the upper limit reported for a 15 km star, even if there is no internal heating (see Table 2). In contrast, the initial heat content of our nonstandard cooling model gives a surface temperature at 10^4 yr more than four times lower than the lower limit for an 8 km star (see Table 3). Ögelman and Zimmerman (1989) concluded that the observed radiation could be due to internal heating and nonstandard cooling. In their analysis, they tacitly assumed that the Vela pulsar is in the photon cooling era. However, our nonstandard cooling model with the surface temperature they reported is still in the neutrino cooling era (see Table 1). Our evolutionary calculations also indicate that if it has nonstandard cooling, the Vela pulsar is still cooling primarily via neutrino emission at the present epoch, even if it has no internal heating (see Table 3); with internal heating, neutrino cooling becomes more important. Assuming thermal balance in the neutrino cooling era and using the observed deceleration rate, our nonstandard cooling model has a surface temperature close to the value reported by Ögelman and Zimmerman only if the internal heating rate is orders of magnitude larger than the maximum rate currently expected (see eq. [39]).

Alpar *et al.* (1984*a*) have estimated that the current internal temperature of the Vela pulsar is $1.5 \pm 1 \times 10^7$ K, based on their interpretation of its postglitch pulse frequency behavior. The upper end of this range is an order of magnitude lower than the internal temperature at 10^4 yr predicted by our standard cooling model without internal heating (see Table 2). For our nonstandard cooling model, this range of temperatures implies J values in the range $10^{41}\text{–}10^{46}$ g cm^2 rad s^{-1} ($\bar{\omega} \sim 0.1\text{–}1000$ rad s^{-1}), again illustrating the sensitivity of the inferred value of J to the internal temperature, in the neutrino cooling era (see eq. [36]).

PSR 1055−52.—This pulsar was one of the brightest X-ray sources found in the initial survey of rotation-powered pulsars made with the *Einstein Observatory* (Cheng and Helfand 1983). *EXOSAT* observations have been reported by Brinkmann and Ögelman (1987). If the observed flux is produced by thermal emission from the stellar surface, the distance is 920 pc, and the radius of the star is in the range 8–15 km, the effective surface temperature is estimated to be $7.1 \pm 1.2 \times 10^5$ K, corresponding to a bolometric luminosity in the range $1\text{–}7 \times 10^{32}$ ergs s^{-1}. The initial heat content of both our standard and nonstandard cooling models produces surface temperatures at 5×10^5 yr, the pulsar's characteristic age, that are $\lesssim 10\%$ of the temperature reported by Brinkmann and Ögelman (see Tables 2 and 3). For nonstandard cooling, the pulsar is still in the neutrino cooling era (see Table 1). The observed deceleration rate gives a surface temperature $\sim 30\%$ of that reported, for $J \approx 2 \times 10^{43}$ g cm^2 rad s^{-1} ($\bar{\omega} \approx 10$ rad s^{-1}); heating rates

orders of magnitude greater than in current models would be required to produce a surface temperature close to the temperature cited (see eq. [39]). For standard cooling, the pulsar is cooling primarily via photon emission (see Table 1). For the observed crustal deceleration rate, our standard cooling model gives a surface temperature comparable to the value reported, if $J \approx 3 \times 10^{44}$ g cm^2 rad s^{-1} or $\bar{\omega} \approx 1$ rad s^{-1} (see eq. [49]). Brinkmann and Ögelman concluded that the observed emission could not be due to internal heating because they assumed $J \lesssim 10^{43}$ g cm^2 rad s^{-1}.

PSR 1509−58.—The X-ray flux from this pulsar in the diffuse supernova remnant MSH 15−52 corresponds to a luminosity in the *Einstein Observatory* band of 5×10^{34} ergs s^{-1} and is ∼100% pulsed with a period of 150 ms (Seward and Harnden 1982). If this radiation is thermal emission from the stellar surface, the surface temperature is $\sim 2.5 \times 10^6$ K. The true age of this pulsar is somewhat uncertain, since its characteristic age is 1.5×10^3 yr whereas the diffuse remnant surrounding it appears to be $\sim 10^4$ yr old. However, evolutionary calculations indicate that the pulsar is still in the neutrino cooling era for any age in this range. This is also implied by the reported surface temperature (see Table 1). The surface temperature of our standard cooling model without internal heating is ∼30% lower at 1.5×10^3 yr than the temperature inferred from the X-ray observations (see Table 2). For the observed deceleration rate, the surface temperature of the standard cooling model is roughly consistent with the observed temperature for any superfluid differential angular momentum in the range expected (see eq. [37]). Our nonstandard cooling model with the highest rate of internal heating currently thought possible ($J \sim 2 \times 10^{43}$ g cm^2 rad s^{-1} or $\bar{\omega} \sim 10$ rad s^{-1}) has a surface temperature an order of magnitude lower than the temperature inferred from observation.

PSR 1642−03.—Using the *Einstein Observatory*, Helfand, Chanan, and Novick (1980) have set an upper limit of 3.5×10^5 K on the surface temperature of this pulsar, for interstellar neutral hydrogen densities less than 1.0 cm^{-3}. The pulsar has a characteristic age of 3.5×10^6 yr. If standard cooling applies, it is in the photon cooling era (see Table 1). For the observed deceleration rate, our standard cooling model is consistent with the temperature limit if $J < 3 \times 10^{44}$ g cm^2 rad s^{-1} ($\bar{\omega} < 1$ rad s^{-1}). Our nonstandard cooling model is consistent with the reported upper limit for all of the energy dissipation rates considered here.

PSR 1706−16.—Helfand, Chanan, and Novick (1980) also placed an upper limit of 4×10^5 K on the surface temperature of this pulsar, for interstellar neutral hydrogen densities less than 1.0 cm^{-3}. Its characteristic age is 1.6×10^6 yr. If standard cooling applies, it is also in the photon cooling era. Our standard cooling model is consistent with the observed deceleration rate and temperature limit of $J < 4 \times 10^{44}$ g cm^2 rad s^{-1} ($\bar{\omega} < 1$ rad s^{-1}). Again, our nonstandard cooling model is consistent with the reported upper limit for all of the energy dissipation rates considered here.

PSR 1929+10.—This pulsar, which has a characteristic age of 3×10^6 yr, has been observed by Alpar *et al.* (1987) using *EXOSAT*. These authors place an upper limit of 1.9×10^5 K on the effective surface temperature and an upper limit of 10^{30} ergs s^{-1} on the photon luminosity, if the star has a radius of 10 km. These upper limits imply that the pulsar is well into the photon cooling era, for standard cooling, or just entering it, for nonstandard cooling (see Table 1). Assuming that this pulsar is in thermal balance in the photon cooling era, the reported upper limits and the observed deceleration rate imply $J < 6 \times 10^{42}$ g cm^2 rad s^{-1} for both our standard and nonstandard cooling models. The corresponding limits on $\bar{\omega}$ are $\bar{\omega} < 0.02$ rad s^{-1} and $\bar{\omega} < 4$ rad s^{-1}. Alpar *et al.* (1987) found $\bar{\omega} \lesssim 0.7$ rad s^{-1} because they assumed $I_s = 10^{43}$ g cm^2 and $R = 10$ km.

Kristian *et al.* (1989; see also Middleditch *et al.* 1989) have recently reported detection of 2 kHz optical pulsations at the location of supernova 1987A. If this detection is confirmed and the pulsation frequency proves to be the rotation frequency of a neutron star, the implications for neutron star structure and evolution (as well as many other aspects of neutron stars, see Alpar *et al.* 1989) will be profound. The requirement that the star be dynamically stable rules out relatively stiff equations of state, like that used in constructing model 1, while the requirement that the maximum mass of a slowly rotating star be greater than 1.44 $M_\odot$ (the mass of PSR 1913+16) rules out very soft equations of state (Friedman, Ipser, and Parker 1989; Shapiro, Teukolsky, and Wasserman 1989). The additional requirement that the star be secularly stable against nonaxisymmetric perturbations probably rules out all previously proposed neutron matter equations of state, although a very narrow range of new neutron matter equations of state may be allowed (Friedman, Ipser, and Parker 1989; Kluźniak *et al.* 1989). This detection may therefore indicate the existence of neutron stars with condensed pion or quark cores, or even stars made of strange or abnormal matter (Frieman and Olinto 1989; Haensel and Zdunik 1989). Such stars would exhibit nonstandard cooling.

To summarize, our standard cooling model is consistent with observed and inferred temperatures and temperature upper limits for most pulsars. An exception is the Vela pulsar, which has an apparent surface temperature about 50% lower than that of our standard cooling model without heating at 10^4 yr; the internal temperature of Vela inferred by Alpar *et al.* from their vortex creep model of postglitch relaxation is an order of magnitude lower than the internal temperature of our standard cooling model without internal heating at this age. Where it is consistent with existing temperature estimates and upper limits, our standard cooling model implies or permits superfluid differential motions ranging from very small ($\bar{\omega} \sim 0.01$ rad s^{-1}) to very large ($\bar{\omega} \sim 10$ rad s^{-1}).

Our nonstandard cooling model is consistent with four temperature upper limits, but is inconsistent with four surface temperature estimates and the internal temperature of the Crab pulsar inferred by Alpar *et al.* from their vortex creep model. Where it is consistent with observed or inferred temperature constraints, the nonstandard cooling model generally allows large superfluid differential rotations ($\bar{\omega} \sim 10$ rad s^{-1}). The one exception is PSR 0525+21, where our nonstandard cooling model is consistent with the internal temperature inferred by Alpar *et al.* from their vortex creep model only if the mean differential rotation of the frictionally coupled superfluid is small ($\bar{\omega} \ll 1$ rad s^{-1}). Alternatively, it may be that only a small fraction of the superfluid in PSR 0525+21 is frictionally coupled to the rest of the star.

V. CONCLUDING REMARKS

We have shown that the thermal evolution predicted by current models of the superfluid-crust interaction is quite different from the thermal evolution predicted by models without internal heating and previous models of heating. Heating rates near the maximum expected in current models significantly

increase the photon luminosity of the star in the neutrino cooling era and dramatically alter the thermal evolution in the photon cooling era. Even quite small heating rates can greatly increase the temperature in the photon cooling era, qualitatively changing the thermal evolution.

Standard cooling models are consistent with current pulsar temperature estimates and upper limits, except those for the Vela pulsar, which are lower than predicted. The superfluid differential rotations typically implied or allowed by such models range from very small to very large, depending on the pulsar. Nonstandard cooling models are consistent with existing temperature upper limits, even for high rates of internal heating. However, these models predict surface temperatures lower than those reported in several pulsars, even if internal heating rates are very high.

Exponential decay of the external braking torque causes the surface temperature of an internally heated neutron star to fall exponentially. However, the available evidence suggests that torque decay occurs only after $\sim 10^7$ yr. If so, neutron stars as old as 10^6 yr may have surface temperatures as high as 6×10^5 K, and may therefore be detectable by *AXAF* (see Wilson 1987).

The thermal flux from nearby old pulsars may also be observable in the extreme UV using future instruments. For example, even a very low internal energy dissipation rate will heat a star with standard cooling to a surface temperature $\sim 10^5$ K at 10^6 yr, producing a photon luminosity $\sim 10^{30}$ ergs s^{-1}. Observations of such pulsars would provide important information about the internal structure of neutron stars and the electrical, thermal, and dynamical properties of neutron star matter.

It is a pleasure to thank M. A. Alpar and R. I. Epstein for many useful discussions. We also thank V. Petrosian, P. Sturrock, and R. Wagoner for their warm hospitality at Stanford University where part of this work was carried out. F. K. L. also thanks the John Simon Gaggenheim Memorial Foundation for generous support. This research was supported in part by NASA grants NAGW 1583 (at Illinois) and NGR 05-020-668 (at Stanford) and NSF grants PHY 86-00377 (at Illinois) and PHY 86-03273 (at Stanford).

REFERENCES

Ainsworth, T., Pines, D., and Wambach, J. 1989, *Phys. Letters A*, in press.
Alpar, M. A. 1977, *Ap. J.*, **213**, 527.
Alpar, M. A., Anderson, P. W., Pines, D., and Shaham, J. 1984*a*, *Ap. J.*, **276**, 325.
———. 1984*b*, *Ap. J.*, **278**, 791.
Alpar, M. A., Brinkmann, W. K. Kızıloğlu, Ü., Ögelman, H., and Pines, D. 1987, *Astr. Ap.*, **177**, 101.
Alpar, M. A., Cheng, K. S., and Pines, D. 1989, *Ap. J.*, submitted.
Alpar, M. A., Cheng, K. S., Pines, D., and Shaham, J. 1988, *M.N.R.A.S.*, **233**, 25.
Alpar, M. A., Fushiki, I., Lamb, F. K., Miller, G. S., Park, M.-G., and Pines, D. 1989, *Nature*, **338**, 295.
Alpar, M. A., Langer, S. A., and Sauls, J. A. 1984, *Ap. J.*, **282**, 533.
Alpar, M. A., Nandkumar, R., and Pines, D. 1985, *Ap. J.*, **288**, 191.
Alpar, M. A., and Pines, D. 1989, in *Timing Neutron Stars*, ed. H. Ögelman and E. P. J. van den Heuvel (Dordrecht: Kluwer), p. 441.
Alpar, M. A., and Sauls, J. A. 1988, *Ap. J.*, **327**, 723.
Anderson, P. W., Alpar, M. A., Pines, D., and Shaham, J. 1982, *Phil. Mag. A.*, **45**, 227.
Anderson, P. W., and Itoh, N. 1975, *Nature*, **256**, 25.
Baym, G. 1981, *Ap. J.*, **248**, 767.
Baym, G., and Pethick, C. J. 1979, *Ann. Rev. Astr. Ap.*, **17**, 415.
Baym, G., Pethick, C. J., Pines, D., and Ruderman, M. A. 1969, *Nature*, **224**, 872.
Baym, G., Pethick, C. J., and Sutherland, P. G. 1971, *Ap. J.*, **170**, 299.
Bildsten, L., and Epstein, R. I. 1989, *Ap. J.*, in press.
Blair, D. G., and Candy, B. N. 1989, in *Timing Neutron Stars*, ed. H. Ögelman and E. P. J. van den Heuvel (Dordrecht: Kluwer), p. 609.
Blandford, R. D., Applegate, J. H., and Hernquist, L. 1983, *M.N.R.A.S.*, **204**, 1025.
Boynton, P. E. 1981, in *IAU Symposium* **95**, *Pulsars*, ed. R. Wielebinski and W. Sieber (Dordrecht: Reidel), p. 279.
Boynton, P. E., and Deeter, J. E. 1979, in *Compact Galactic X-Ray Sources*, ed. F. K. Lamb and D. Pines (Urbana: University of Illinois), p. 168.
Boynton, P. E., Deeter, J. E., Lamb, F. K., Zylstra, G., Pravdo, S. H., White, N. E., and Wood, K. 1984, *Ap. J. (Letters)*, **283**, L53.
Brinkmann, W., and Ögelman, H. 1987, *Astr. Ap.*, **182**, 71.
Candy, B. N., and Blair, D. G. 1986, *Ap. J.*, **307**, 535.
Chen, J. M. C., Clark, J. W., Krotscheck, E., and Smith, R. A. 1986, *Nucl. Phys. A.*, **451**, 509.
Cheng, A. F., and Helfand, D. J. 1983, *Ap. J.*, **271**, 271.
Córdova, F. A., Hjellming, R. M., Mason, K. O., and Middleditch, J. 1989, *Ap. J.*, submitted.
Deeter, J. E., Boynton, P. E., Lamb, F. K., and Zylstra, G. 1989, *Ap. J.*, **336**, 376.
Demianski, M., and Proszynski, M. 1983, *M.N.R.A.S.*, **202**, 437.
Dewey, R. J. 1989, in *Timing Neutron Stars*, ed. H. Ögelman and E. P. J. van den Heuvel (Dordrecht: Kluwer), p. 573.
Downs, G. S. 1981, *Ap. J.*, **249**, 687.
———. 1982, *Ap. J. (Letters)*, **257**, L67.
Epstein, R. I. 1988, *Phys. Rept.*, **163**, 155.
Epstein, R. I., and Baym, G. 1988, *Ap. J.*, **328**, 680.
Feibelman, P. J. 1971, *Phys. Rev. D*, **4**, 1589.
Flowers, E., and Itoh, N. 1979, *Ap. J.*, **230**, 847.
———. 1981, *Ap. J.*, **250**, 750.
Frieman, J. A., Ipser, J. R., and Parker, L. 1989, preprint.
Frieman, J. A., and Olinto, A. V. 1989, *Nature*, submitted.
Ginzburg, V. L., and Kirzhnits, D. A. 1965, *Soviet Phys. JETP*, **20**, 136.
Glen, G., and Sutherland, P. G. 1980, *Ap. J.*, **239**, 671.
Greenstein, G. 1975, *Ap. J.*, **200**, 281.
———. 1976, *Ap. J.*, **208**, 836.
———. 1979, *Ap. J.*, **231**, 880.
Gudmundsson, E. H., Pethick, C. J., and Epstein, R. I. 1982, *Ap. J. (Letters)*, **259**, L19.
———. 1983, *Ap. J.*, **272**, 286.
Gunn, J. E., and Ostriker, J. P. 1970, *Ap. J.*, **160**, 979.
Haensel, P., and Zdunik, J. L. 1989, *Nature*, submitted.
Harding, D., Guyer, R. A., and Greenstein, G. 1978, *Ap. J.*, **222**, 991.
Harnden, F. R., Jr., Grant, P. D., Seward, F. D., and Kahn, S. M. 1985, *Ap. J.*, **299**, 828.
Harnden, F. R., Jr., and Seward, F. D. 1984, *Ap. J.*, **283**, 279.
Helfand, D. J. 1983, in *IAU Symposium* **101**, *Supernova Remnants and Their X-Ray Emission*, ed. P. Gorenstein and J. Danziger (Dordrecht: Reidel), p. 471.
Helfand, D. J., Chanan, G. A., and Novick, R. 1980, *Nature*, **283**, 337.
Hernquist, L. 1985, *M.N.R.A.S.*, **213**, 313.
Hernquist, L., and Applegate, J. H. 1984, *Ap. J.*, **287**, 244.
Hoffberg, M., Glassgold, A. E., Richardson, R. W., and Ruderman, M. 1970, *Phys. Rev. Letters*, **24**, 175.
Jones, P. B. 1988, *M.N.R.A.S.*, **235**, 545.
Kluźniak, W., Lindblom, L., Michelson, P., and Wagoner, R. V. 1989, *Nature*, submitted.
Kristian, J., Pennypacker, C. R., and Middleditch, J., *et al.* 1989, *Nature*, **338**, 234.
Lamb, F. K. 1985, in *Galactic and Extragalactic Compact X-Ray Sources*, ed. Y. Tanaka and W. H. G. Lewin (Tokyo: Institute of Space and Astronautical Science), p. 19.
Lohsen, E. H. G. 1981, *Astr. Ap. Suppl.*, **44**, 1.
Lyne, A. G., Manchester, R. N., and Taylor, J. H. 1985, *M.N.R.A.S.*, **213**, 613.
Lyne, A. G., Pritchard, R. S., and Smith, F. G. 1988, *M.N.R.A.S.*, **233**, 667.
Manchester, R. N., and Taylor, J. H. 1977, *Pulsars* (San Francisco: Freeman).
Maxwell, O. V. 1978, Ph.D. thesis, State University of New York at Stony Brook.
Middleditch, J., Pennypacker, C. R., and Kristian, J., *et al.* 1989, *Nature*, submitted.
Migdal, A. B. 1959, *Nucl. Phys.*, **13**, 655.
Nandkumar, R. 1985, unpublished.
Narayan, R. 1987, *Ap. J.*, **319**, 162.
Nomoto, K., and Tsuruta, S. 1981, *Ap. J. (Letters)*, **250**, L19.
———. 1987, *Ap. J.*, **312**, 711.
Ögelman, H., and Zimmermann, H.-U. 1989, *Astr. Ap.*, submitted.
Pacini, F. 1967, *Nature*, **216**, 567.
Packard, R. E. 1972, *Phys. Rev. Letters*, **28**, 1080.
Pandharipande, V. R., Pines, D., and Smith, R. A. 1976, *Ap. J.*, **208**, 550.

Pandharipande, V. R., and Smith, R. A. 1975, *Nucl. Phys. A.*, **237**, 507.
Pines, D., and Alpar, M. A. 1985, *Nature*, **316**, 27.
Pines, D., Shaham, J., Alpar, M. A., and Anderson, P. W. 1980, *Prog. Theor. Phys. Suppl.*, **69**, 376.
Radhakrishnan, V., and Manchester, R. N. 1969, *Nature*, **222**, 228.
Reichley, P. E., and Downs, G. S. 1969, *Nature*, **222**, 229.
Richardson, M. B., Van Horn, H. M., Ratcliff, K. F., and Malone, R. C. 1982, *Ap. J.*, **255**, 624.
Romani, R. W. 1987, *Ap. J.*, **313**, 718.
Ruderman, M. A. 1976, *Ap. J.*, **203**, 213.
Sauls, J. A. 1989, in *Timing Neutron Stars*, ed. H. Ögelman and E. P. J. van den Heuvel (Dordrecht: Kluwer), p. 457.
Seward, F. D. 1987, in *IAU Symposium* **125**, *The Origin and Evolution of Neutron Stars*, ed. D. J. Helfand and J.-H. Huang (Dordrecht: Reidel), p. 99.
Seward, F. D., and Harnden, F. R., Jr. 1982, *Ap. J. (Letters)*, **256**, L45.
Shaham, J. 1977, *Ap. J.*, **214**, 251.
Shapiro, S. L., Teukolsky, S. A., and Wasserman, I. 1989, *Nature*, submitted.
Takatsuka, T. 1984, *Progr. Theor. Phys.*, **71**, 1432.
Tsuruta, S. 1986, *Comments Ap.*, **11**, 151.
Tsuruta, S., and Cameron, A. G. W. 1965, *Nature*, **207**, 364.
Van Riper, K. A. 1988, *Ap. J.*, **329**, 339.
Van Riper, K. A., and Lamb, D. Q. 1981, *Ap. J. (Letters)*, **244**, L13.
Ventura, J. 1989, in *Timing Neutron Stars*, ed. H. Ögelman and E. P. J. van den Heuvel (Dordrecht: Kluwer), p. 491.
Wilson, A. S. 1987, *Ap. Letters Comm.*, **26**, 99.

FREDERICK K. LAMB: Department of Physics, University of Illinois at Urbana-Champaign, 1110 W. Green Street, Urbana, IL 61801

NORIAKI SHIBAZAKI: Department of Physics, Rikkyo University, Nishi-Ikebukuro, Tokyo 171, Japan